

LOWER CRUSTAL MATERIALS EXPOSED IN THE APOLLO BASIN REVEALED USING MOON MINERALOGY MAPPER (M³) DATA. N.E. Petro¹, J. Sunshine², C. Pieters³, R. Klima^{3,7}, J. Boardman⁴, S. Besse², J. Head³, P. Isaacson³, L. Taylor⁵, S. Tompkins⁶. ¹NASA/GSFC, Code 698, Greenbelt, MD (Noah.E.Petro@nasa.gov), ²University of Maryland, ³Brown University, ⁴AIG LLC, ⁵University of Tennessee, ⁶DARPA, ⁷JHU/APL.

Introduction: The Apollo Basin is a 480 km diameter, pre-Nectarian, multi-ring basin located within the large South Pole-Aitken Basin (SPA) [1-3]. Multispectral data from both Galileo and Clementine showed that the composition of materials in Apollo is distinct compared to its surroundings [4-7]. To the south and west of Apollo are mafic (largely noritic and basaltic) materials associated with the interior of SPA [7, 8]; to the north and east are SPA basin massifs [9] and anorthositic materials associated with the Feldspathic Highlands Terrane [10]. Using data from the Moon Mineralogy Mapper (M³), an imaging spectrometer flown on the Chandrayaan-1 mission, we identify both noritic and anorthositic mineralogies exposed within Apollo. The distribution of these materials within Apollo relative to materials in SPA is then used to reconstruct a possible crustal stratigraphy in for this region.

Previous Interpretations of Apollo Compositions: Both the Galileo and Clementine missions revealed the Apollo Basin to be spectrally and geologically unique. Using Galileo SSI data, the interior of Apollo was found to be similar in albedo, visible spectral slope, and mafic mineral content to areas in SPA west of Apollo, suggesting that Apollo exposed a thick and extensive unit of mafic crustal material [4]. Clementine UVVIS data were later used to discover anorthositic materials in the rings of Apollo which are amongst the few probable exposures of such compositions in SPA [5, 7, 11]. These low-Fe materials were initially interpreted to have formed as a result of a differentiated SPA-melt sheet [11].

M³ Data: The M³ is an imaging spectrometer with high spatial (140-280 m) and spectral resolution covering the wavelength range from 430-3000 nm. Data taken in the lower resolution global mode covering the Apollo basin was collected during the second optical period of operations from both 100 and 200 km orbits. Preliminary mosaics of all M³ data at a 10X reduced spatial resolution of 1.4 km/pixel have been created in a simple cylindrical projection. Shown in Figure 1 is a subset of the mosaic for the area surrounding Apollo. Spectra shown here have a correction applied to suppress high-frequency calibration artifacts and are truncated at 2600 nm.

Compositional Analysis: The interior of Apollo is only partially flooded by mare basalts (Figure 1) allowing much of the interior of the basin to be exposed. Illustrated in Fig. 1C is a color composite sensitive to mafic composition. This color composite is used to identify the range of materials within Apollo, greens are suggestive of low-Ca bearing pyroxenes (noritic materials), oranges

and yellows are indicative of high-Ca pyroxenes (basalts and gabbros), and blues represent anorthositic or low-FeO bearing materials.

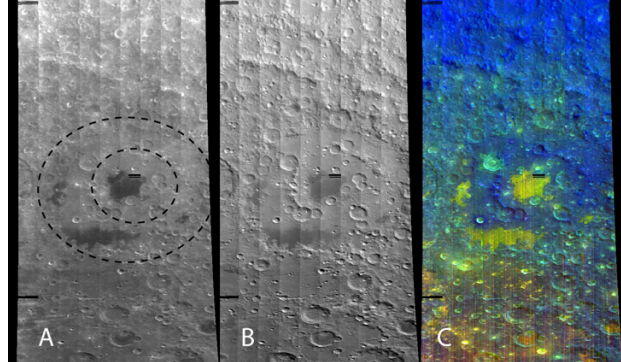


Figure 1. Mosaiced M³ data at 1.4 km/pixel from second optical period in simple cylindrical projection. A) 750 nm albedo image of Apollo Basin region. Main (480 km diam.) and inner rings (240 km diam.) of the basin are identified by dashed circles [3]. B) Long wavelength (2936 nm) image, which is sensitive to surface topography. C) Color composite image with R = Integrated Band Depth (IBD) of the 1000 nm band, G = IBD of the 2000 nm band, and B = 1580 nm reflectance.

Anorthositic Materials: As shown with Clementine data [5, 7], portions of the interior of Apollo appear to contain anorthositic materials. These areas appear as blue in Fig. 1C. Averaged spectra of areas on the Apollo inner ring are shown in Fig. 2. It is important to note that for wavelengths longer than 2200 nm, there is an added thermal component to all spectra [12]. In addition to the inner ring, much of the floor of Apollo between the inner and main ring is composed of “anorthositic” soils. Also included in Fig. 2 is a spectrum of a mature highland soil from an area outside SPA (north of Apollo). The “anorthositic” materials associated with the interior of Apollo are all spectrally distinct from the mature highland soil. Most notably, Apollo soils and ring material all have weak absorption features near 1000 nm, suggesting that the materials in Apollo are enriched in iron relative to mature highlands.

Noritic Materials: Outside Apollo, SPA soils over large areas are generally noritic (greens in Fig. 1c) [7, 8]. Within Apollo, however, soils are generally “anorthositic” while the exposures of noritic material are confined to several, but not all, craters (greens in Fig. 1C). Spectra from craters of various sizes across the basin interior (Fig. 3) reveal that the non-mare mafic materials have short wavelength 1000 nm band centers near or below 950 nm, consistent with low-Ca pyroxenes and suggestive of a noritic composition [see 13, 14]. A spec-

trum of fresh basalt in Mare Orientale is presented for comparison. This spectrum exhibits a longer wavelength 1000 nm absorption feature due to the presence of abundant high-Ca pyroxene. Also in Fig. 3 is a spectrum from the central peak of Antoniadi, a 143 km diameter crater in SPA, which is consistent with a low-Ca pyroxene.

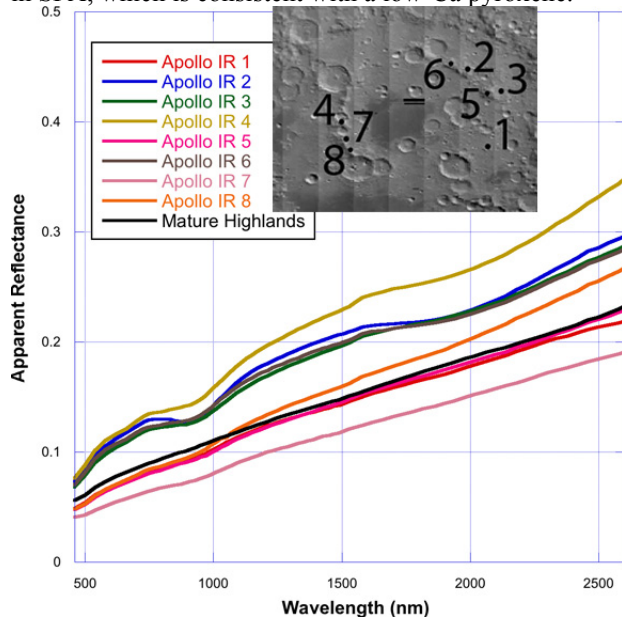


Figure 2. M^3 3×3 averaged spectra extracted from around the inner ring of Apollo. The mature highlands spectrum was extracted from an area north of Apollo, outside of SPA. The inset image indicates where the eight Apollo spectra were extracted.

Summary and Conclusions: The Apollo Basin has two unique compositions exposed in its interior. The general composition of its interior is “anorthositic,” except that unlike typical farside feldspathic highlands, the “anorthositic” materials in Apollo exhibit weak 1000 nm absorption features, suggesting that they contain some component of mafic minerals. These “anorthositic” materials stand in stark contrast to the strong mafic enhancement pervasive across SPA [7]. Previous interpretations of the unusual “anorthositic” material in Apollo suggested that it formed as the result of a differentiated SPA melt sheet that was subsequently exposed by the formation of Apollo [11]. While noritic material in SPA are common and have been interpreted as being SPA impact melt material [7, 8], the very thin (<10 km) crust in with Apollo [15] may hint at another source for the Apollo noritic material.

One possible origin for these unusual materials is that the “anorthositic” and noritic materials in Apollo represent remnant primary crust of the region and not necessarily a secondary crust (impact melt). Because much of the anorthositic upper crust was excavated by SPA’s formation [16] and a noritic melt sheet likely did cover the SPA interior (including the Apollo target region) [17], Apollo would have likely excavated through a SPA melt-sheet, which would be thinner at the margins of the

basin. Apollo’s size suggests that it could have excavated ~30 km below the target surface [18], implying that Apollo might have excavated through SPA impact melt and exposed the underlying crustal materials. The “anorthositic” material in the Apollo inner ring might represent a more mafic, lower portion of the crust. Subsequent impacts in Apollo exposed deeper, noritic lower crustal materials. If the noritic materials are from the lower crust, then they are of a different provenance than the impact melt noritic materials across SPA. Preliminary analyses suggest that noritic materials outside of Apollo (e.g., Antoniadi in Fig. 3) are indeed a different composition than the noritic materials in Apollo.

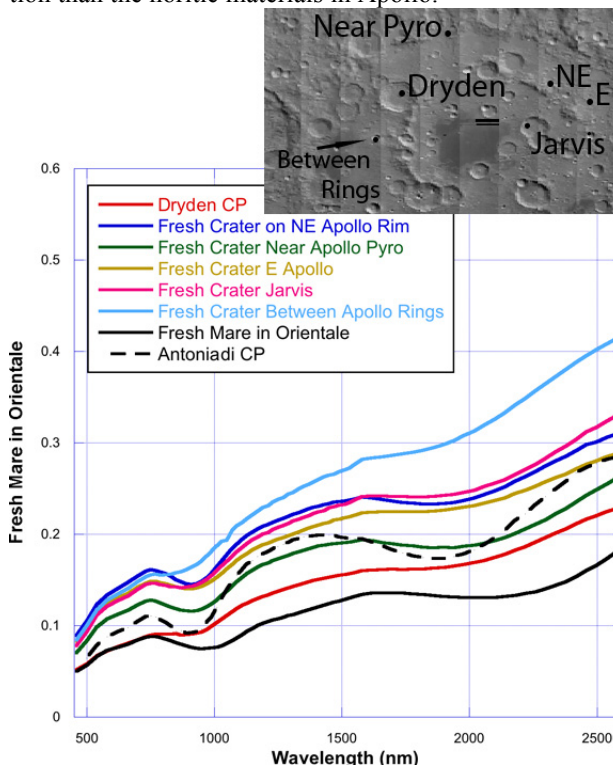


Figure 3. M^3 3×3 averaged spectra extracted from locations across the interior of Apollo. The fresh mare spectrum was extracted from Mare Orientale and dashed spectrum is from the central peak of Antoniadi. The inset image illustrates where Apollo spectra were extracted.

References: [1] Wilhelms, D. E., (1987) *The Geologic History of the Moon*, 327 p. [2] Stuart-Alexander, D. E., (1978) Geologic map of the central far side of the Moon, I-1047. [3] Namiki, N., et al., (2009) *Science*, 323, 900-905. [4] Head, J. W., et al., (1993) *JGR*, 98, 17,149-117,181. [5] Morrison, D. A., et al., (1997), *Lunar Planet. Sci.*, Abst. #987-988. [6] Petro, N. E. and C. M. Pieters, (2002) *Lunar Planet. Sci.*, 33, 1848. [7] Pieters, C. M., et al., (2001) *JGR*, 106, 28001-28022. [8] Nakamura, R., et al., (2009) *Geophys. Res. Lett.*, 36, L22202. [9] Garrick-Bethell, I. and M. T. Zuber, (2009) *Icarus*, 204, 399-408. [10] Jolliff, B., et al., (2000) *JGR*, 105, 4197-4216. [11] Morrison, D. A., (1998), LPSC 29, Abst. #1657. [12] Pieters, C. M., et al., (2009) *Science*, 326, 568-572. [13] Klima, R., et al., (2009), LPSC 41. [14] Klima, R. L., et al., (2007) *MAPS*, 42, 235-253. [15] Ishihara, Y., et al., (2009) *GRL*, 36, 19202. [16] Wieczorek, M. A. and R. J. Phillips, (1999) *Icarus*, 139, 246-259. [17] Warren, P. H., et al., (1996) *GSA Special Paper*, 307, 105-124. [18] Cintala, M. J. and R. A. F. Grieve, (1998) *MAPS*, 33, 889-912.